Dynamic Contact Angle Studies of Self-Assembled Thin Films from Fluorinated Alkyltrichlorosilanes[1]

Mark J. Pellerite,*,† Erika J. Wood,† and Vivian W. Jones‡

3M Company, 3M Center 201-1W-28, St. Paul, Minnesota 55144

Received: October 16, 2001; In Final Form: February 10, 2002

Dynamic contact angle studies on self-assembled thin films from $C_7F_{15}CH_2OCH_2CH_2CH_2SiCl_3$ reveal a range of interesting behavior. Solution-based processing conditions have been identified that allow preparation of essentially monolayer films on quartz exhibiting water adv/rec contact angles of 119/104 ± 2° and extremely low contact angle hysteresis (hexadecane adv/rec = 74/70°, heptane adv/rec = 56/55°) with hydrocarbon liquids. This compound provides an example of a fluorinated trichlorosilane that is able to deliver low-hysteresis films by deposition at room temperature. Adsorption of silane oligomers, formed by hydrolysis and condensation reactions in solution, was also found to occur, slower than but competitive with monolayer formation. This process became more significant as dip coating times increased. Ellipsometric data on silicon wafers confirmed that film thicknesses increased with dip time, while AFM imaging showed that the oligomeric material was deposited in the form of particulates. The effects of this process on water dynamic contact angles are discussed. We also compare contact angles on these films with those on films prepared from $C_nF_{2n+1}CH_2CH_2SiCl_3$ (n = 6, 8, 10) and draw some conclusions regarding structure−property effects in these systems. Finally, we propose a mechanism that can account qualitatively for the bulk of the results observed here. Its central feature is reaction of the fluorinated alkyltrichlorosilane with surface-adsorbed water to yield a self-assembled monolayer consisting of silanetriol molecules hydrogen-bonded to the substrate. Effects of high humidity aging on dynamic contact angles of these films suggest that they are at most only lightly cross-linked when prepared under conditions utilized here.

Introduction

Alkylsilanes $RSiX_3$ (R = alkyl, X = Cl, alkoxy) on siliceous surfaces and other substrates represent one of the most extensively investigated classes of self-assembling monolayer systems. Since the pioneering work of Sagiv and co-workers,[2] virtually every tool available to the surface chemist has been brought to bear in the study of these systems.[3−35] The picture that has emerged[2,10,25] regarding the structure of these monolayers revolves around a two-dimensional cross-linked alkylsiloxane network, formed by hydrolysis of the trichlorosilane and condensation of the resulting silanol groups, partially bound to the substrate through additional condensation with surface silanols (Figure 1), although the extent and distribution of siloxane linkages is currently subject to debate. This view has recently been challenged, however,[36] so despite the voluminous literature in this area, research is extremely active and basic mechanistic questions remain to be answered.

Fluorinated alkylsilanes have been somewhat less well-studied[48] than their hydrocarbon counterparts, even though such materials are finding application as low-surface-energy films for optical substrates[49] and lubricating treatments for microelectromechanical systems (MEMS) devices.[37] For instance, dynamic contact angles in these films are not well characterized, and most of the work reported to date has involved silanes of the general structure **1**; little systematic data exist on structure−

$$C_nF_{2n+1}CH_2CH_2SiCl_3$$
1; n = 6, 8, 10

property relationships and the effect on film properties of the linking group structure between the perfluoroalkyl segment and the silyl headgroup.[22,34,38,45−47]

This study presents results from dynamic contact angle measurements on self-assembled films derived from fluorinated trichlorosilane **2** on quartz. Contact angle data before and after

$$C_7F_{15}CH_2OCH_2CH_2CH_2SiCl_3$$
2

aging in dry and humid environments, along with ellipsometry and AFM data on coated silicon wafers, are discussed within the framework of a mechanistic hypothesis for the formation and structure of these self-assembled thin films. Also presented are some limited dynamic contact angle data on films from **1** obtained on quartz under the same conditions, to probe the significance of structure−property interactions in these films. Where possible, we attempt to place the data from this study, and the picture that emerges therefrom, in the context of results from previous work[22,37] on mechanism and structure in fluorinated alkyltrichlorosilane self-assembly. We prefer the general term "thin films" because, as we show, any description of self-assembled films from **2** strictly in terms of monolayers is not only overly confining, but at times incorrect.

Experimental Section

Materials. All solvents and reagents were standard commercial grade and used as received. Methyl perfluorobutyl ether

* To whom correspondence should be directed. E-mail: mjpellerite1@mmm.com. Fax: 651-737-5335.

† Advanced Materials Technology Center.

‡ Corporate Analytical Technology Center.

10.1021/jp013820m CCC: $22.00
Published on Web 04/09/2002

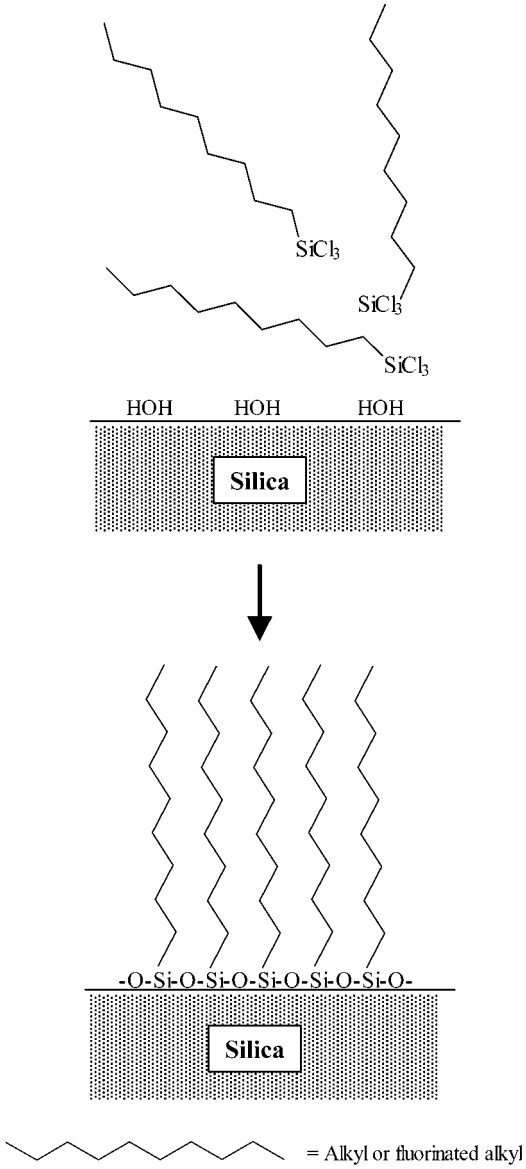

Figure 1. Simplified schematic illustration of self-assembled monolayer formation from alkyltrichlorosilane or fluorinated alkyltrichlorosilane on siliceous surface.

(HFE-7100), 1*H*,1*H*-pentadecafluorooctanol ($C_7F_{15}CH_2OH$), and bis(divinyltetramethyldisiloxane)platinum(0) (23 wt % Pt in siloxanes) were obtained from 3M Co. The fluorinated alcohol used here was a ~70:30 mixture of linear and branched C_7F_{15} chains by ^{19}F NMR analysis.[50] Silanes **1** (n = 6, 8) were obtained from Gelest, Inc., Tullytown, PA, while 1*H*,1*H*,2*H*-perfluoro-1-dodecene ($C_{10}F_{21}CH{=}CH_2$) was obtained from Lancaster Synthesis, Windham, NH. Water-saturated heptane was prepared by adding 0.1 g of water to a 1 L bottle of commercial reagent-grade heptane, shaking the mixture, and allowing it to stand overnight before use. When decanting the heptane for use in preparation of coating solutions, care was taken not to sample the water phase. Water (18.2 MΩ) for contact angle measurements was drawn from a Millipore deionized water filtration system. Hexadecane was of commercial anhydrous grade and used as received.

Trichloro-3-(1*H*,1*H*-pentadecafluorooctyloxy)propylsilane ($C_7F_{15}CH_2OCH_2CH_2CH_2SiCl_3$, 2). To a stirred solution of 124 g (0.31 mol) of 1*H*,1*H*-pentadecafluorooctanol and 62 g (0.51 mol) of allyl bromide in 1240 g of dimethyl sulfoxide at room temperature was added dropwise a solution of 28.1 g of (0.43 mol) potassium hydroxide in 35 g of water. The mixture was allowed to stir for 4 h, during which time it split into two immiscible liquid phases. The lower layer was isolated in a separatory funnel and washed three times with water to remove any remaining solvent. The crude product was dried over anhydrous magnesium sulfate, filtered, and vacuum distilled to yield 103 g (76% yield) of 1*H*,1*H*-pentadecafluorooctyl allyl ether, $C_7F_{15}CH_2OCH_2CH{=}CH_2$, bp 88−89 °C/30 mmHg. The product exhibited ^1H and ^{19}F NMR spectra consistent with this structure. This procedure was found to afford higher, more consistent yields than the method reported in the literature.[51]

The above allyl ether was converted to silane **2** by heating in a screw-top vial at 60 °C overnight a mixture of allyl ether, 20% molar excess of trichlorosilane, and 100 ppm Pt catalyst (added as a 1 wt % solution of bis(divinyltetramethyldisiloxane)-Pt(0) in dichloromethane). The crude reaction product was purified by vacuum distillation to afford trichlorosilane **2**, bp 110−117 °C/2 mmHg (lit.[51] 125 °C/7.5 mmHg), in yields of typically 70−85%. NMR (in $CDCl_3$): ^1H, δ 1.5 (m, 2H); δ 1.9 (m, 2H); δ 3.6 (t, J = 6 Hz, 2H); δ 3.9 (t, J = 14 Hz, 2H); ^{13}C, δ 20.8, δ 22.9, δ 68.1, δ 73.4; ^{29}Si, δ 13.1. HRMS: obsd, m/z 538.9491 $(M - Cl)^+$; calc for $C_{11}H_8Cl_2F_{15}OSi$, 538.9481. The product was contaminated by <5% β-isomer, $C_7F_{15}CH_2OCH_2$-$CH(CH_3)SiCl_3$. The major low-boiling byproduct was C_7F_{15}-$CH_2OCH{=}CHCH_3$ (mixture of cis and trans isomers), formed by rearrangement of the starting allyl ether. Yields of this byproduct varied from run to run in the range of 15−30%.

Trichloro-1*H*,1*H*,2*H*,2*H*-perfluorododecylsilane, $C_{10}F_{21}CH_2$-CH_2SiCl_3. A screw-top vial equipped for magnetic stirring was charged with 5.46 g of 1*H*,1*H*,2*H*-perfluoro-1-dodecene ($C_{10}F_{21}CH{=}CH_2$, 0.01 mol), 0.38 g of 1 wt % solution of bis-(divinyltetramethyldisiloxane)Pt(0) in dichloromethane, and 1.59 g (0.012 mol) of trichlorosilane. The vial was capped and the mixture stirred until the exotherm had subsided. The reaction mixture was then heated in an oil bath at 60 °C for 24 h, and the product, a solid at room temperature, was isolated by bulb-to-bulb vacuum distillation. The yield of $C_{10}F_{21}CH_2CH_2SiCl_3$ was 6.13 g (90%), bp 100−105 °C/0.05 mmHg (lit.[52] 85−86 °C/0.6 mmHg). Analysis of the product by ^1H NMR showed <0.5% residual olefin and no detectable β-isomer.

Substrates. Quartz rods (2 mm diameter) were obtained from the 3M Co. Central Research Glass Shop and cut to 55 mm length. Silicon wafers were ⟨100⟩ orientation, P-type, boron-doped, 75 mm diameter, obtained from Silicon Sense, Inc. (Nashua, NH.)

Substrate and Film Preparation. *Substrate Cleaning.* Quartz rods were degreased by immersion for several minutes in an ultrasound bath containing a 1:1 (v/v) mixture of ethanol and chloroform, then allowed to dry in air. Final cleaning was accomplished by either 10 min exposure in an air plasma (Harrick (Ossining, NY) PDC-3xG plasma cleaner/sterilizer, set at high power) or 5 min exposure in a home-built UV/ozone chamber. Silicon wafers were cut into quarters and cleaned by 5 min exposure in the UV/ozone chamber. These treatments were found to yield hydrophilic substrates giving water contact angles of essentially zero.

Preparation and Characterization of Self-Assembled Films. Immediately after cleaning, substrates were allowed to stand for 20 min in a 100% relative humidity chamber, then removed and immediately dipped for the desired exposure time (0.5−60 min) in a freshly prepared solution of 0.1 or 0.3 wt % fluorinated trichlorosilane in heptane (1.2 or 3.6 mM **2**). Self-assembled films made under optimized conditions utilized 0.1 wt % solutions of silane in water-saturated heptane; as-received

heptane was also used in some experiments as noted in the text. All treatments were performed at room temperature. Samples were found to be autophobic and emerged completely dry from the coating solutions, except for those processed at the longest dip coating times for which only partial autophobicity was observed. Contact angle measurements were performed on fresh coating samples with no additional processing, except for coated silicon wafers that were measured before and after solvent rinsing, as noted below. Wilhelmy measurements were also repeated on coated quartz rod samples after storage in 0 or 100% relative humidity chambers for various periods.

Film Characterization. *Contact Angle Measurements.* Dynamic contact angles on coated quartz rod substrates were measured using a Cahn Instruments (Madison, WI) DCA-322 Wilhelmy balance and a stage speed of 90 μ/s. In this technique,[53] a microbalance measures the force exerted on a vertically mounted sample by the wetting meniscus as the liquid reservoir is raised and lowered over about the first 1 cm of the sample length. Using instrument software, a least-squares fit of the linear regions of a plot of advancing and receding meniscus force versus stage displacement was extrapolated to zero depth of immersion (to eliminate buoyancy effects), and the advancing and receding forces at this point, F^{adv}_{zdi} and F^{rec}_{zdi}, were determined. These values were then used to compute the dynamic contact angles θ_{adv} and θ_{rec} using eq 1[53a,b] with

$$F_{zdi} = P\gamma \cos\theta \qquad (1)$$

experimentally determined values of the sample perimeter P and the surface tension γ of the wetting liquid. P was calculated from $P = \pi d$, where d is the diameter of the quartz rod measured with a micrometer. Surface tensions were measured using a freshly cleaned, hydrophilic quartz rod and eq 1 assuming $\cos\theta = 1$. Three complete advancing/receding contact angle cycles were always run to assess film stability upon immersion in the wetting medium, and generally two sets of measurements were run to generate stabilized samples for oil contact angle determinations (see text). A fresh sample of wetting liquid was used for each three-cycle measurement. Surface tensions of water, hexadecane, and heptane wetting liquids were always measured at the start of each session as an internal check of the system. Measured values were typically within 0.5 dyn/cm of the accepted literature[54] values. Static and dynamic contact angles on coated silicon wafers were measured using an AST Products (Billerica, MA) VCA-2500XE video contact angle (VCA) apparatus. Estimated uncertainties in the contact angles were $\pm 2°$ for the Wilhelmy measurements, $\pm 1°$ for static and advancing VCA measurements, and $\pm 2°$ for receding VCA measurements.

Ellipsometry Measurements on Silicon Wafers. Using a Gaertner (Skokie, IL) L116A single-wavelength ellipsometer operating at 6328 Å and 70° incident angle, ellipsometric parameters Ψ and Δ were measured on the same four spots before and after coating. Film thicknesses were determined from these values[55] using software supplied with the instrument, a three-layer model (air/film/substrate), and film refractive index $n_f = 1.36$ (the value measured for the neat trichlorosilane **2**). Ellipsometric measurements were made before and after vigorous agitation of the coated samples submerged for 1 min in a beaker of methyl perfluorobutyl ether, then in a beaker of 2-propanol.

AFM Measurements. Coated silicon wafer samples that had been rinsed as described above were imaged using tapping-mode atomic force microscopy on a Nanoscope IIIa multimode scanning probe microscope (Digital Instruments, Santa Barbara, CA). Probe tips (Olympus, Japan) with a nominal force constant of 40 N/m were used. Typical amplitude dampening settings for imaging were 0.75 (set-point amplitude/free amplitude) with a scan rate of 1 Hz.

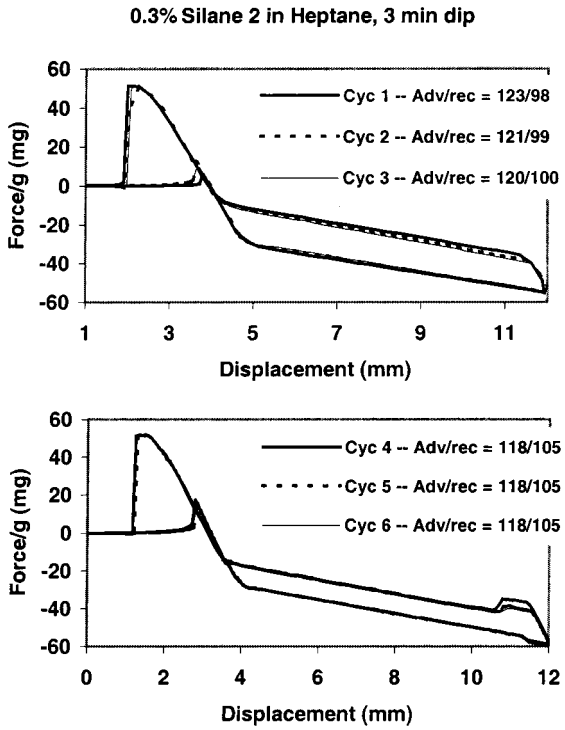

Figure 2. Wilhelmy dynamic contact angle data for first two sets of three adv/rec cycles for self-assembled film from silane **2** on quartz rod, 0.3 wt % silane in heptane, 3 min dip.

Results and Discussion

Ultimate Contact Angles for Self-Assembled Films from Silane 2 on Quartz. Water contact angles, particularly receding values, on quartz rods treated with silane **2** were found to be strongly dependent on coating conditions. Some of this dependence was systematic, such as that on dip time in the coating solution (vide infra), while much of it could be capricious and difficult to reproduce. The procedure outlined in the Experimental Section represents the combination of conditions that in our hands yielded the most consistent results. Fresh solutions of 0.1 wt % silane in water-saturated[28] heptane, UV/ozone cleaning, and preconditioning of cleaned substrates in 100% relative humidity before coating[56] all contributed to improved reproducibility. Additional treatments after coating such as rinsing with water or solvents, or heating,[6,15] provided no benefit. Under these optimized conditions, 1−3 min dip times gave the highest, most consistent water contact angles. Also, in general, contact angles would vary during the first set of Wilhelmy cycles and stabilize during the second set, as illustrated in Figure 2. A proposed origin of this effect is discussed below. Table 1 shows the water dynamic contact angles obtained for stabilized coatings prepared under these conditions on quartz, along with hexadecane and heptane contact angles obtained from further measurements on previously stabilized samples.

While extremely low hysteresis ($\theta_{adv} - \theta_{rec}$)[57] on the order of a few degrees or less could be obtained with the oils, about 15° was the lowest that could be obtained with water. Nevertheless, the water receding angle of 104° (averaged over many runs) observed here is among the highest reported in the literature for self-assembled fluorinated alkyltrichlorosilane films on

TABLE 1: Dynamic Contact Angles for Stabilized Self-Assembled Films from Fluorinated Trichlorosilanes on Quartz Rods

	adv/rec CA (deg)[a]		
compound	water	hexadecane	heptane
$C_7F_{15}CH_2OCH_2CH_2CH_2SiCl_3$	119/104	74/70	56/55
$C_6F_{13}CH_2CH_2SiCl_3$	113/94		
$C_8F_{17}CH_2CH_2SiCl_3$	119/100		62/59
$C_{10}F_{21}CH_2CH_2SiCl_3$	118/95		64/58

[a] Scatter in contact angle measurements was typically ±2°.

smooth[58] substrates. This value is somewhat lower than the 110° reported for solvent-cast and annealed films of a fluoroalkyl acrylate polymer,[59] and significantly lower than the 116° reported for a vacuum-deposited $C_{20}F_{42}$ thin film[60] and the 117° exhibited by a $C_{10}F_{21}(CH_2)_{11}SH$ self-assembled monolayer on gold.[61]

For water and hydrocarbon wetting liquids, we observed a correlation between advancing contact angle and hysteresis: Water, which gave the highest advancing angles, also yielded the highest hysteresis. Analogous behavior has been noted on thin films prepared using monofunctional fluoroalkylsilanes.[40] Fadeev and McCarthy,[62a] in an extensive study of wettabilities on grafted films of hydrocarbon trialkylsilanes on silicon, report similar results for measurements with water, methylene iodide, and hexadecane. However, hysteresis was similar with the latter two liquids, despite methylene iodide giving larger contact angles. We observed consistently larger hysteresis with hexadecane ($\gamma = 27.5$ dyn/cm[54]) than with heptane ($\gamma = 20.1$ dyn/cm[54]). The correlation between advancing or static contact angles and wetting liquid surface tension is of course well-known and manifests itself in the Zisman plot.[63] However, it is not obvious that such a general relationship should also exist between contact angle hysteresis and surface tension. Perhaps this is indicative of less-than-perfect monolayers, since contact angles on high-quality self-assembled thiol monolayers on gold typically show low hysteresis with both water and oils. One example of this is provided by recent data of Fukushima and co-workers[61] for monolayers prepared from $C_{10}F_{21}(CH_2)_{11}SH$ on gold. These films gave adv/rec contact angles of 83/75° with hexadecane and 122/117° with water. While this hexadecane hysteresis of 8° is only slightly larger than that (4°) observed here for **2** films on quartz, the water hysteresis is substantially lower (5° vs 15° in our study.) This could suggest that water contact angle hysteresis is the more sensitive probe of monolayer quality, but we also note with caution that this comparison involves completely different amphiphile/substrate systems.

Finally, we examined the effects of adding small amounts of alkylamines to coating solutions of **2**, as well as preconditioning cleaned quartz rod substrates in an atmosphere of ammonia before dip coating. The former caused severe problems with coating solution stability, while the latter had no discernible effect on contact angles of the resulting self-assembled films. Tripp and Hair[44] reported that amines can enhance formation and properties of films prepared from (3,3,3-trifluoropropyl)-trichlorosilane on silicon wafers. However, we found no evidence for such effects operating in our system.

Dependence of Water Dynamic Contact Angles on Dip Time. Coating time exerted dramatic effects on water dynamic contact angles of self-assembled thin films derived from silane **2**. Illustrative data are shown in Figure 3. Both advancing and receding angles rose rapidly with dip time, the receding angle going through a maximum around 1−3 min and dropping off at longer times, while the advancing angle continued to increase and leveled off after ∼10 min.

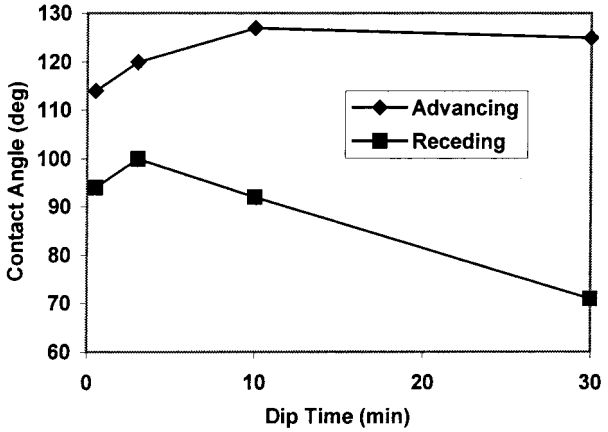

Figure 3. Water advancing and receding contact angles for self-assembled films from silane **2** on quartz rods, 0.3 wt % in heptane, as a function of dip time.

TABLE 2: Ellipsometric Thickness and Water Contact Angles for Self-Assembled Films[a] from Silane 2 on Silicon Wafers before and after Solvent Rinsing

	thickness (Å)[b]		static/adv/rec water CA (deg)	
dip time (min)	before rinse	after rinse	before rinse	after rinse
1	19	15	116/121/108	115/121/110
3	26	17	115/121/110	115/123/107
10	32	19	111/122/104	113/123/103
30	44	27	108/122/81	113/127/95
60	∼80	45	111/123/87	122/131/89

[a] Wafers cleaned and prepared as described in text; coatings prepared by dipping for indicated times in 0.1 wt % **2** in water-saturated heptane. Rinses done in methyl perfluorobutyl ether then 2-propanol. [b] Scatter in ellipsometric thicknesses was ±1 Å for dip times of 1−3 min, ±2−4 Å for longer times. Thickness for 60 min dip unrinsed film was difficult to reproduce.

An analogous dependence was observed by Menawat and co-workers[64] in a study of several hydrocarbon silanes, in which silane concentration was varied at fixed dip time. Their observed increase in hysteresis was attributed to multilayer adsorption at higher concentrations, with the maximum in receding angle thought to coincide with the highest-quality, best-packed monolayer. For our fluorinated system, although monolayer formation from monomeric silane appears to be the faster process, self-assembly does not simply stop at the monolayer; instead, hydrolysis and oligomerization of the silane in solution and adsorption of oligomeric siloxane species[37] also occurs in competition with monolayer formation. As discussed below, we believe that this phenomenon is responsible for the contact angle dependence on dip times seen in Figure 3 and Table 2.

Oligomer adsorption can account for our observation that for short dip times, the water contact angles changed during the first set of three DCA cycles on a fresh sample, finally stabilizing during the second set (Figure 2). We believe this is due to removal of small amounts of weakly bound oligomers by the water meniscus during the first set of cycles. At short dip times, the levels of adsorbed oligomers are low, and the excess material can still be removed by rinsing, unlike on films prepared at longer dip times. This effect is also seen in ellipsometry data on coated silicon wafers (vide infra). However, the amounts of material involved here appear to be too small to detect in surface tension measurements on water samples used in the contact angle determinations; no reduction from the value for pure water was ever observed.

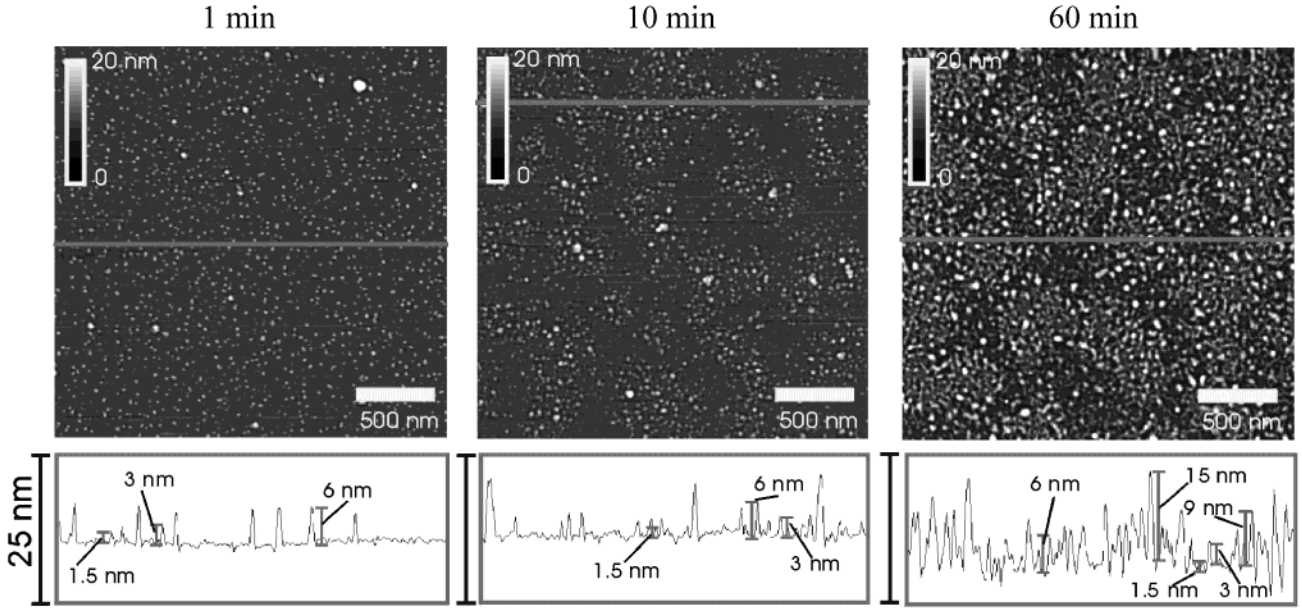

Figure 4. AFM images and profile analyses (along the indicated horizontal lines) of self-assembled films from silane **2** on silicon wafers prepared at various dip times (0.1 wt % silane in water-saturated heptane) and solvent rinsed as described in the text.

Additional evidence for the connection between contact angle hysteresis and oligomer adsorption can be found in the contact angle and ellipsometry data for self-assembled films from silane **2** on silicon wafers, as shown in Table 2. Compiled there are static, advancing, and receding water contact angles and ellipsometric film thicknesses on wafer samples treated at dip coating times ranging from 1 to 60 min, both before and after rinsing with methyl perfluorobutyl ether (a good solvent for the fluorinated silane and oligomers) and 2-propanol. Here again, as was seen in the contact angle data on quartz rods, receding contact angles decreased with increasing dip times; the ellipsometric data show clearly that film thicknesses also increased. Even 1 min dip time gave unrinsed films in excess of one monolayer thick, suggesting that oligomer adsorption occurs at a rate competitive with that for monolayer formation. Note also that the maximum receding contact angles on rinsed films occurred for those prepared at short dip times and giving thicknesses in the monolayer range[65] of 15−17 Å. Furthermore, since rinsing of short dip time samples yielded films of essentially monolayer thickness, this implies that the bulk of the excess material was weakly adsorbed and easily removed by rinsing. On the other hand, while rinsing of longer dip time samples removed a portion of the film thickness in excess of one monolayer, it did not remove all of it, nor did it restore the high receding contact angles seen on samples prepared at short dip times. This underscores the role of the oligomers in the contact angle dependence on dip time. It also suggests that oligomers adsorbed at long dip times are more strongly bound (perhaps covalently, via condensation of oligomer silanol groups with silanols exposed at defects in the monolayer) than those adsorbed at short dip times. Or, this could be a manifestation of oligomer molecular weights increasing (and hence their solubility in the rinse solvent dropping) as reaction time increases. In any case, taken together, our data provide good support for the main features of the above mechanism. Also, they emphasize the importance of obtaining receding contact angle measurements when comparing a series of film samples. Table 2 shows that static and advancing angles do not always reveal the full story, and receding angles are much more sensitive to subtle changes in film structure.[53d]

AFM images on the above silicon wafer samples shed some light on the form taken by the adsorbed oligomeric material. Figure 4 shows images of solvent-rinsed wafers dip coated for 1, 10, and 60 min (ellipsometric thicknesses 16, 21, and 43 Å, respectively.) It is clear that the film thickness in excess of one monolayer is caused by adsorption of small particulate islands that are even found at short dip times. Profile analysis of the images shows a distribution of 15−60 Å feature heights at 1 min dip time, 15−90 Å at 10 min, and up to 150 Å at 60 min. In addition to becoming more numerous, the particulates appear to be growing as dip time increases.

Adsorption of particulates was also observed recently by Bunker and co-workers[37] in AFM imaging of self-assembled films from silane **1** ($n = 8$) delivered from isooctane, but there are significant differences in behavior between the two cases. For instance, in Figure 4 the particulates appear to be adsorbing in quasi-cluster type structures at long dip times. This was not observed[37] for **1**, where the particulate distribution appeared to be fairly random. Origins of this difference are unknown but are under study. Also, the features observed by Bunker and co-workers were significantly larger than those seen here, being up to 300 nm in width and 25 nm in height.[37] This could arise from differences in solubility of the two silanes in the solvents employed for film formation. Bunker and co-workers present convincing evidence for formation of aggregated, inverse micellar structures in solutions of silane **1** in isooctane. Although silane **2** would exhibit better solubility than **1** in hydrocarbon media due to the lower fluorine content, it is entirely likely that aggregated structures form in the silane solutions in wet heptane used in this work. Indeed, the solutions do show a Tyndall effect,[66] suggesting the presence of colloidal species. We have not undertaken the light scattering experiments that would be necessary to confirm this and explore the system further. Also, our coatings are prepared on a time scale significantly shorter than that required for trichlorosilane hydrolysis and particulate nucleation in the experiments of Bunker and co-workers.[37] A detailed analysis of the AFM images obtained for self-assembled films from silane **2** is beyond the scope of this paper and is the subject of ongoing investigation. Nevertheless, the images support the notion that adsorption of excess material is occurring

in this self-assembly process and show that such adsorption does not involve continuous buildup of smooth films. At this point, we believe that the surface roughness introduced by these particulates is responsible for the significant hysteresis in the water dynamic contact angles, since the hysteresis and the density of adsorbed particles both increase with dip time. One might also argue that the increase in hysteresis can be viewed within the framework of "molecular scale roughness" advanced by Fadeev and McCarthy.[62a] In this case, the roughness would be caused by adsorbed or grafted oligomeric segments. However, their work showed water contact angles relatively independent of molecular scale roughness,[62b] whereas Table 2 shows a large increase in hysteresis at longer dip times. Therefore, we favor the interpretation that the contact angle hysteresis in Figure 3 originates from larger-scale (tens of nanometers) roughness induced by adsorption of oligomeric particulate species.

Comparison of Water and Oil Contact Angles for Films from Silanes 1 and 2. Some interesting features emerge when comparing dynamic contact angles for the four compounds **1** ($n = 6, 8, 10$) and **2** (Table 1). For instance, water receding contact angles for **1** passed through a maximum for $n = 8$, while $n = 6$ also gave lower advancing angles than its homologues. Thus, among **1** ($n = 6, 8, 10$), $n = 8$ gave the highest-quality films[38] for depositions at room temperature.

Dynamic contact angle behavior of silanes **1** ($n = 8$) and **2** also makes for an interesting comparison. Although the water advancing angles were essentially identical, we obtained higher receding angles for **2** under all conditions investigated, including many side-by-side runs with both compounds under identical conditions. This is surprising in view of the mixture of linear and branched perfluoroheptyl segments as well as the linking group ether oxygen in **2**, both of which might be expected to adversely affect contact angle behavior. Differences also appeared in the heptane data, with **2** giving near zero hysteresis and lower angles. Rondelez and co-workers reported low hysteresis for films prepared from **1** ($n = 8, 10$) by dip coating at subambient temperatures and stated that "good grafting with fluorinated silanes requires low temperatures of reaction."[22] Silane **2** is an example of a fluorinated silane that can assemble at room temperature into films showing almost no contact angle hysteresis with heptane.

In their same 1994 study, Rondelez and co-workers[22] proposed the existence of a critical temperature T_c for silane film formation, below which optimum packing of the monolayer can be achieved. This behavior was thought to be related to the transition between liquid expanded and liquid compressed states in Langmuir monolayers. The value of T_c is a function of silane structure; for hydrocarbon silanes, T_c increases with increasing alkyl chain length. In this work, both hydrocarbon and fluorocarbon silanes (specifically, **1** ($n = 8, 10$)) showed lower alkane contact angle hysteresis when coated below T_c (which is below room temperature for the fluorinated silanes[22]).

The above observation that **2** gives lower hysteresis than **1** ($n = 8$) when coated at room temperature seems inconsistent with the Rondelez picture. Given the correlation between T_c and chain length for hydrocarbon silanes, we expect silane **2**, with its branched perfluoroalkyl chain content and the flexibilizing ether oxygen, to have a lower T_c than the linear and more highly fluorinated **1** ($n = 8$). Thus, at room temperature, **2** should be further above T_c than **1** ($n = 8$); with respect to film properties, one would predict a result opposite that observed.

We account for this behavior by proposing that the more flexible molecule, **2**, can assemble and pack more easily than **1**

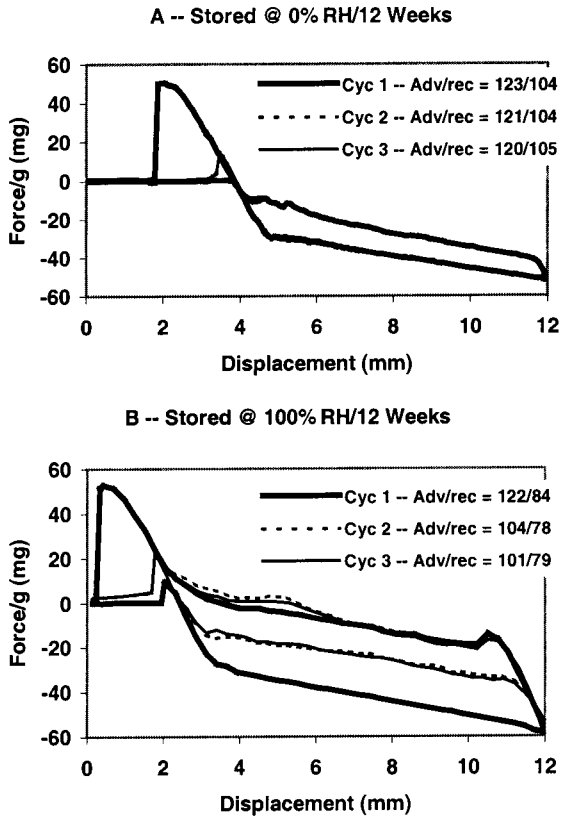

Figure 5. Wilhelmy water dynamic contact angle data on two quartz rods, bearing self-assembled films from silane **2**, after storage under conditions indicated. These two rod samples were prepared using identical conditions and both gave adv/rec = 120/104 initially after stabilization (see text.)

($n = 8$) and give more uniform film coverage. The branched isomer content in **2** is perhaps the origin of the lower alkane contact angles relative to those for **1** ($n = 8$). Stated differently, hysteresis may be more related to substrate coverage and film uniformity, while chain structure differences show up in alkane (but not water) advancing angles. Results supporting this notion were also obtained by Fadeev and co-workers[40] in dynamic contact angle studies on a series of monofunctional fluoroalkylsilanes bearing linear and branched terminal fluorochemical segments. They reported higher water advancing and receding contact angles and lower pentadecane contact angles for branched fluoroalkyl segments relative to their linear counterparts. Such a picture is also consistent with the assertion put forth by Fadeev and McCarthy[62a] that organic wetting liquids can penetrate some types of hydrocarbon silane monolayers and sample other structural features of the silane alkyl chain, whereas water does not. Traditionally, this is thought not to be the case with crystalline monolayers exhibiting high packing density,[31,62a] but these shorter-chain fluorinated silane films may fall short in fulfilling these requirements. Indeed, **1** ($n = 8$) has yielded amorphous monolayers under some conditions.[21]

Effects of Storage on Water Dynamic Contact Angles in Self-Assembled Films from 2. The contact angles shown in Table 1 for stabilized films from trichlorosilane **2** and **1** ($n = 8$) on quartz rods were not stable to storage at room temperature under high humidity. Bunker and co-workers[37] and de Boer and co-workers[67] have also pointed out that high humidity storage results in degradation of wetting and lubricative properties of silicon wafers treated with self-assembled films derived from silane **1** ($n = 8$.) Figure 5 illustrates this behavior for films from silane **2**. It shows water dynamic contact angle data on two stabilized film samples, taken after storage in 0 or 100%

relative humidity (RH) for 12 weeks. These two samples were prepared under identical conditions, and when fresh, both gave water adv/rec contact angles of 120/104. While 0% RH storage did essentially nothing to these values, 100% RH induced profound changes. The first-cycle advancing angle was largely unchanged from that for the fresh sample, but all subsequent advancing and receding angles were significantly lower. This pattern appeared consistently, although the exact magnitude of the contact angle changes and the storage time needed to produce them could vary from sample to sample. Second and third cycle advancing angles would typically drop 5−15°, while the receding angles could drop 10−20°, relative to those for the fresh coating. Some samples exhibited these changes after only 1−2 weeks' storage at high humidity, while others took longer. The large drop in advancing angles between the first and second cycle indicates significant changes occurring in the film upon exposure to liquid water.

Proposed Mechanism for Self-Assembly of Fluorinated Alkyltrichlorosilane Films. Much of the literature on alkyltrichlorosilane self-assembly on silica utilizes a model in which condensation of silanols leads to formation of cross-linked siloxane networks, covalently bound to the substrate through occasional condensation with surface silanol groups.[2,10,25] Recently, Stevens[36] emphasized that long-chain alkyl groups are too bulky to allow silanol condensation and construction of well-ordered, two-dimensionally cross-linked films, because their van der Waals cross-sectional radii are larger than the Si−O bond length. One of the basic assumptions that has guided research in this area for more than 20 years is thus called into question.

This situation can only be worse for fluorinated alkylsilane-derived films, since perfluoroalkyl segments exhibit larger cross-sectional areas than their hydrocarbon analogues.[19,21] Thus, it appears extremely unlikely that these systems, including those of the present study, can be forming the classical two-dimensional cross-linked siloxane network with vertically oriented, ordered fluorochemical chains.

We propose a mechanistic picture (Figure 6) for formation of self-assembled films from fluorinated alkyltrichlorosilanes on quartz that takes this view into account while also rationalizing much of the experimental results described here. In this mechanism, the active amphiphilic species is the silanetriol $R_fSi(OH)_3$, formed by hydrolysis of the trichlorosilane with surface-adsorbed water.[56] The silanetriol can self-assemble into immobilized monolayer films stabilized by hydrogen bonding with the silica substrate and van der Waals interactions between the fluorochemical groups. It is this construction that we believe gives rise to the films displaying the minimum contact angle hysteresis discussed earlier. This mechanism is similar to that which has appeared in the literature[17,20,22,28,29,37,44,55] many times, except without the extensive condensation and cross-linking generally assumed to occur. Within this framework, and as proposed by Bunker and co-workers,[37] the use of water-saturated heptane probably facilitates coating formation by preventing dissolution of the adsorbed water film into an anhydrous coating medium. Simultaneously, and consistent with other observations,[37,68] the trichlorosilane can react in a competitive process with water in the solvent to eventually yield condensed oligomeric species that can also adsorb to the surface and to the monolayer as contact times with the solution become long (>1 min).

Our experimental data also indicate that, if formed, this arrangement of self-assembled silanetriols in low-hysteresis films is not stable to exposure to 100% RH, although it can be

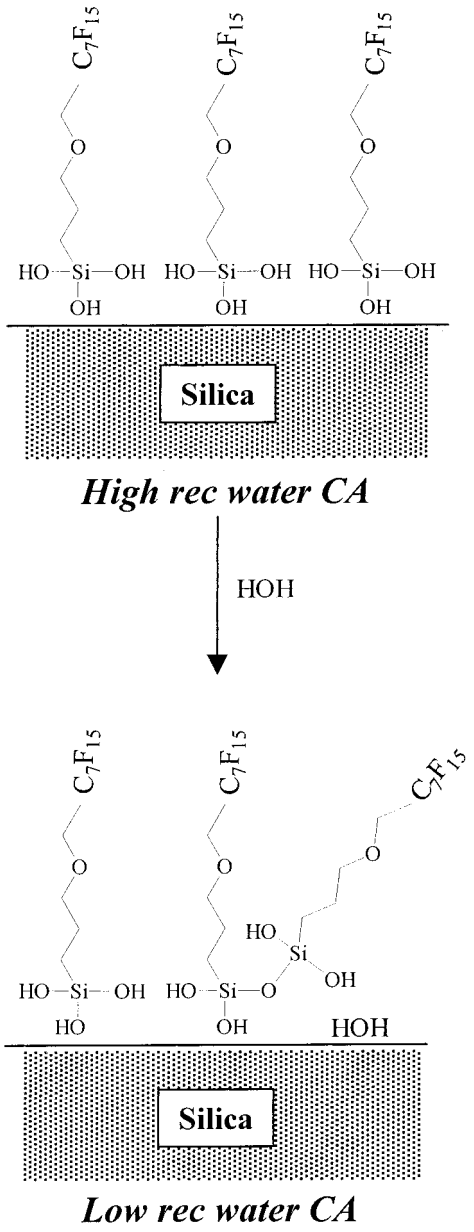

Figure 6. Schematic illustration of proposed mechanism for humidity-induced degradation of water dynamic contact angles for self-assembled films from fluorinated trichlorosilanes such as **2**.

under dry conditions. We suggest that the contact angle degradation[71] that occurs upon exposure of the low-hysteresis films to high humidity is due to disruption, by gaseous water, of the hydrogen bonding between silanetriol and substrate. Under humid conditions, water can penetrate the monolayer film and displace the silanetriol from the surface; these species are then free to condense with other neighboring silanetriols, generating regions of disordered material and leading to greatly reduced receding contact angles and unstable advancing values (Figures 5b and 6). An alternative mechanism, suggested by a referee, involves an initial monolayer with disordered headgroups and some siloxane cross-links; upon exposure to humidity, these hydrolyze, leading to film degradation.[69] In either case, the changes in advancing angles from first to second cycle[71] may suggest further hydration of the quartz surface and disruption of the coating upon immersion in liquid water.

This mechanistic hypothesis raises a number of basic questions that we are not able to answer at this point. Issues of chain packing density, siloxane bond formation, and the role of the

substrate (quartz and silicon may not behave identically due to different levels of surface silanol and adsorbed water; these could affect film properties in as yet undertermined ways) have yet to be sorted out and can provide the basis for future investigations. For instance, detailed AFM analysis could in principle address questions of packing density and chain order, as well as providing a tool for examining structural effects of film exposure to high humidity. The humidity-induced changes we are proposing may be detectable by AFM. Infrared spectroscopy may provide data with which to assess the role of siloxane bond formation,[17,18,44,70] both between molecules and with the substrate, in these self-assembled films, and perhaps allow the above two mechanistic hypotheses for humidity-induced film degradation to be distinguished. At present we have no information on the importance of condensation of silanetriols with each other (cross-linking), or with surface silanols to yield covalently surface-bound fluorinated alkylsilanes.[70] These reactions are potential stabilizing mechanisms for the films. If they occur to varying extents in different samples, this could account for the differences we have seen in humidity-induced contact angle changes and the rates at which they occur.

Summary and Conclusions

Dynamic contact angle studies on self-assembled thin films from fluorinated alkyltrichlorosilane **2** reveal a range of interesting behavior. Conditions have been identified that allow preparation of what are believed to be essentially monolayer films on quartz rods exhibiting water advancing/receding contact angles of 119/104 ± 2°; this receding angle is one of the highest yet reported for fluorinated trichlorosilane films on smooth surfaces. Use of dilute (1.2 mM) solutions of silane, water-saturated heptane as the solvent, and short dip times (1−3 min) were critical to the most consistent preparation of films with minimum hysteresis. These films gave even lower contact angle hysteresis with hydrocarbon wetting liquids. Silane **2** is an example of a fluorinated trichlorosilane that is able to deliver low-hysteresis films by deposition at room temperature.

Measurements on films prepared on silicon wafers as a function of dip time showed that advancing angles continued to increase and receding angles decreased as dip times were increased up to 60 min. This behavior appears to arise from adsorption of oligomeric material from solution to yield thicker, less ordered, and rougher films. Ellipsometric data confirmed that film thicknesses increased with dip time, while AFM imaging showed that this excess material was deposited in the form of particulates. Solvent rinsing removed a fraction of this excess material, with this fraction decreasing as dip times increased. Adsorption of oligomeric siloxane particulates has been noted in previous work with other self-assembled trichlorosilane films;[37,68] these results and ours showed qualitative differences that were attributed to different silane solubilities and film preparation time scales.

Comparison of dynamic contact angles for films prepared from silane **2** with those prepared from silane **1** ($n = 8$) revealed some interesting structure−property trends. Films from silane **2** always yielded lower hysteresis under all conditions studied. Water advancing contact angles were similar, but **1** ($n = 8$) gave higher contact angles with hydrocarbon liquids. We propose that these differences arise from enhanced coverage of monolayer films from silane **2** due to the flexibilizing ether linkage, and the branched perfluoroheptyl group content in the trichlorosilane film precursor **2**.

Water dynamic contact angles on self-assembled films from fluorinated trichlorosilanes on quartz were found to be unstable to storage in high humidity conditions. Whereas for fresh samples the advancing and receding values were perfectly stable over three Wilhelmy cycles, after aging in a 100% RH environment the dynamic contact angle behavior changed completely. The first cycle advancing angle was largely unchanged, but subsequent advancing and all receding cycles showed contact angles 10−20° lower than the same sample before aging.[71]

Finally, we propose a mechanism that can account qualitatively for the bulk of these results. The central feature of this mechanism is reaction of the fluorinated alkyltrichlorosilane with surface-adsorbed water to yield a self-assembled thin film consisting primarily of alkylsilanetriol molecules hydrogen-bonded to the substrate. Our results with high humidity aging of these films suggest that the film is at most only weakly cross-linked, although we cannot rule out covalent bonding of some fraction of the adsorbed molecules to each other and the substrate by silanol condensation. Additional work is needed to address the role of siloxane bonding in these films. Of course, this mechanism and the work reported here still leave many questions unanswered. Nevertheless, we hope that it can serve as a guide for additional efforts that will lead to further fundamental understanding of these interesting systems, as well as provide insight into routes to films with enhanced performance in areas such as surface protection and lubrication.

Acknowledgment. Thanks go to Dr. T. D. Dunbar (3M Advanced Materials Technology Center) for ellipsometric assistance; Drs. D. A. Weil and K. A. Thakur (3M Corporate Analytical Technology Center) for mass spectrometric and NMR work, respectively; and Drs. Dunbar, L. D. Boardman, H. E. Johnson, C. R. Kessel, and R. R. Shah (3M Advanced Materials Technology Center) for helpful discussions and critical reading of the manuscript.

References and Notes

(1) A portion of this work was first presented at the 216th National ACS Meeting, Boston, MA, August 1998.

(2) For leading references, see, for instance: (a) Sagiv, J. *J. Am Chem. Soc.* **1980**, *102*, 92−98. (b) Maoz, R.; Sagiv, J. *J. Colloid Interface Sci.* **1984**, *100*, 465−496.

(3) Ulman, A. *An Introduction to Ultrathin Organic Films*; Academic Press: San Diego, CA, 1991.

(4) Brunner, H.; Vallant, T.; Mayer, U.; Hoffmann, H.; Basnar, B.; Vallant, M.; Friedbacher, G. *Langmuir* **1999**, *15*, 1899−1901.

(5) Fontaine, P.; Goldmann, M.; Rondelez, F. *Langmuir* **1999**, *15*, 1348−1352.

(6) Tian, F.; Xiao, X.; Loy, M. M. T.; Wang, C.; Bai, C. *Langmuir* **1999**, *15*, 244−249.

(7) Vallant, T.; Brunner, H.; Mayer, U.; Hoffmann, H.; Leitner, T.; Resch, R.; Friedbacher, G. *J. Phys. Chem. B* **1998**, *102*, 7190−7197.

(8) Vidon, S.; Leblanc, R. *J. Phys. Chem. B* **1998**, *102*, 1279−1286.

(9) Richter, A. G.; Durbin, M. K.; Yu, C.-J.; Dutta, P. *Langmuir* **1998**, *14*, 5980−5983.

(10) Rye, R. R.; Nelson, G. C.; Dugger, M. T. *Langmuir* **1997**, *13*, 2965−2972.

(11) Huang, J. Y.; Song, K. J.; Lagoutchev, A.; Yang, P. K.; Chuang, T. J. *Langmuir* **1997**, *13*, 58−64.

(12) Banga, R.; Yarwood, J.; Morgan, A. M.; Evans, B.; Kells, J. *Thin Solid Films* **1996**, *284−285*, 261−266.

(13) Lobau, J.; Rumphorst, A.; Galla, K.; Seeger, S.; Wolfrum, K. *Thin Solid Films* **1996**, *289*, 272−281.

(14) Takahara, A.; Kojio, K.; Ge, S.-R.; Kajiyama, T. *J. Vac. Sci. Technol. A* **1996**, *14*, 1747−1754.

(15) Calistri-Yeh, M.; Kramer, E. J.; Sharma, R.; Zhao, W.; Rafailovich, M. H.; Sokolov, J.; Brock, J. D. *Langmuir* **1996**, *12*, 2747−2755.

(16) Bierbaum, K.; Grunze, M. *Langmuir* **1995**, *11*, 2143-2150.

(17) Allara, D. L.; Parikh, A. N.; Rondelez, F. *Langmuir* **1995**, *11*, 2357−2360.

(18) Parikh, A. N.; Liedberg, B.; Atre, S. V.; Ho, M.; Allara, D. L. *J. Phys. Chem. B* **1995**, *99*, 9996−10008.

(19) Banga, R.; Yarwood, J.; Morgan, A. M.; Evans, B.; Kells, J. *Langmuir* **1995**, *11*, 4393−4399.

(20) Nakagawa, T.; Ogawa, K.; Kurumizawa, T. *Langmuir* **1994**, *10*, 525−529.

(21) Ge, S.; Takahara, A.; Kajiyama, T. *J. Vac. Sci. Technol. A* **1994**, *12*, 2530−2536.

(22) Brzoska, J. B.; Ben Azouz, I.; Rondelez, F. *Langmuir* **1994**, *10*, 4367−4373.
(23) Fujii, M.; Sugisawa, S.; Fukada, K.; Kato, T.; Shirakawa, T.; Seimiya, T. *Langmuir* **1994**, *10*, 984−987.
(24) Wei, M.; Bowman, R. S.; Wilson, J. L.; Morrow, N. R. *J. Colloid Interface Sci.* **1993**, *157*, 154−159.
(25) Le Grange, J. D.; Markham, J. L.; Kurkjian, C. R. *Langmuir* **1993**, *9*, 1749−1753.
(26) Tripp, C. P.; Hair, M. L. *Langmuir* **1992**, *8*, 1961−1967.
(27) Tripp, C. P.; Hair, M. L. *Langmuir* **1992**, *8*, 1120−1126.
(28) Silberzan, P.; Leger, L.; Ausserre, D.; Benattar, J. J. *Langmuir* **1991**, *7*, 1647−1651.
(29) Angst, D. L.; Simmons, G. W. *Langmuir* **1991**, *7*, 2236−2242.
(30) Kessel, C. R.; Granick, S. *Langmuir* **1991**, *7*, 532−538.
(31) Wasserman, S. R.; Tao, Y.-T.; Whitesides, G. W. *Langmuir* **1989**, *5*, 1074−1087.
(32) DePalma, V.; Tillman, N. *Langmuir* **1989**, *5*, 868−872.
(33) Wasserman, S. R.; Whitesides, G. W.; Tidswell, I. M.; Ocko, B. M.; Pershan, P. S.; Axe, J. D. *J. Am. Chem. Soc.* **1989**, *111*, 5852−5863.
(34) Maoz, R.; Netzer, L.; Gun, J.; Sagiv, J. *J. Chim Phys.* **1988**, *85*, 1059−1065.
(35) Finklea, H. O.; Robinson, L. R.; Blackburn, A.; Richter, B.; Allara, D.; Bright, T. *Langmuir* **1986**, *2*, 239−244.
(36) Stevens, M. *Langmuir* **1999**, *15*, 2773−2778.
(37) Bunker, B. C.; Carpick, R. W.; Assink, R. A.; Thomas, M. L.; Hankins, M. G.; Voigt, J. A.; Sipola, D.; de Boer, M. P.; Gulley, G. L. *Langmuir* **2000**, *16*, 7742−7751.
(38) Hozumi, A.; Ushiyama, K.; Sugimura, H.; Takai, O. *Langmuir* **1999**, *15*, 7600−7604.
(39) Zybill, C. E.; Ang, H. G.; Lan, L.; Choy, W. Y.; Meng, E. F. K. *J. Organomet. Chem.* **1997**, *547*, 167−172.
(40) Fadeev, A. Y.; Soboleva, O. A.; Summ, B. D. *Colloid J.* **1997**, *59*, 222−225.
(41) Hoffmann, P. W.; Stelzle, M.; Rabolt, J. F. *Langmuir* **1997**, *13*, 1877−1880.
(42) Tada, H.; Nagayama, H. *Langmuir* **1994**, *10*, 1472−1476.
(43) Geer, R. E.; Stenger, D. A.; Chen, M. S.; Calvert, J. M.; Shashidhar, R.; Jeong, Y. H.; Pershan, P. S. *Langmuir* **1994**, *10*, 1171−1176.
(44) Tripp, C. P.; Veregin, R. P. N.; Hair, M. L. *Langmuir* **1993**, *9*, 3518−3522.
(45) Lindner, E.; Arias, E. *Langmuir* **1992**, *8*, 1195−1198.
(46) Yanazawa, H.; Matsuzawa, T.; Hashimoto, N. *J. Adhes. Sci. Technol.* **1990**, *4*, 145−153.
(47) Bascom, W. D. *J. Colloid Interface Sci.* **1968**, *27*, 789−796.
(48) See refs 12, 14, 19, 21−23, 31, 32, 34, 37−47.
(49) U. S. Patent 5,851,674 (1999).
(50) For another example where a fluorinated material with this type of isomeric chain distribution has been used in preparation of organic thin films, see: Schmidt, D. L.; DeKoven, B. M.; Coburn, C. E.; Potter, G. E.; Meyers, G. F.; Fischer, D. A. *Langmuir* **1996**, *12*, 518−529.
(51) U. S. Patent 3,012,006 (1961).
(52) Yoshino, N.; Yamamoto, Y.; Hamano, K.; Kawase, T. *Bull. Chem. Soc. Jpn.* **1993**, *66*, 1754−1758.
(53) (a) Tretinnikov, O. N.; Ikada, Y. *Langmuir* **1994**, *10*, 1606−1614. (b) Hayes, R. A.; Ralston, J. *Chem. Australia* **1992**, 524−528. (c) Lander, L. M.; Siewierski, L. M.; Brittain, W. J.; Vogler, E. A. *Langmuir* **1993**, *9*, 2237−2239. (d) Sessile drop measurements of hexadecane contact angles on the rinsed 1 and 3 min coated silicon wafer samples in Table 2 showed hysteresis and contact angle values within a few degrees of those on quartz rods (Table 1). Thus, we did not observe the effect noted by Fukushima and co-workers[61] in which Wilhelmy and sessile drop methods yielded significantly different results. While this was attributed to differences inherent in fabrication of the gold substrates (ref 61,) at least one study (ref 53c) has shown that systematic differences can occur in water contact angles measured with the two techniques. This was not seen in our work, at least to a significant extent. Also, for short dip times (1−3 min), the static water contact angles in Table 2 are in good agreement with those reported (ref 37) for films from **1** ($n = 8$); however, we did not see values approaching 140° at long times as reported there.
(54) Jasper, J. J. *J. Phys. Chem. Ref. Data* **1972**, *1*, 841−1009.
(55) Parikh, A.; Allara, D.; Azouz, I. B.; Rondelez, F. *J. Phys. Chem.* **1994**, *98*, 7577−7590.
(56) A small amount of water adsorbed on the substrate is known (refs 28, 29, and 37) to be essential for formation of high-quality alkyltrichlorosilane films.
(57) Some workers (see, for instance, refs 22 and 31) use ($\cos \theta_{adv} - \cos \theta_{rec}$) to obtain hysteresis values proportional to surface energies.
(58) Values on microstructured surfaces can be much higher due to roughness effects: (a) Öner, D.; McCarthy, T. J. *Langmuir* **2000**, *16*, 7777−7782. (b) Shibuichi, S.; Yamamoto, T.; Onda, T.; Tsujii, K. *J. Colloid Interface Sci.* **1998**, *208*, 287−294.
(59) Katano, Y.; Tomono, H.; Nakajima, T. *Macromolecules* **1994**, *27*, 2342−2344.
(60) Nishino, T.; Meguro, M.; Nakamae, K.; Matsushita, M.; Ueda, Y. *Langmuir* **1999**, *15*, 4321−4323.
(61) Fukushima, H.; Seki, S.; Nishikawa, T.; Takiguchi, H.; Tamada, K.; Abe, K.; Colorado, R.; Graupe, M.; Shmakova, O. E.; Lee, T. R. *J. Phys. Chem. B* **2000**, *104*, 7417−7423.
(62) (a) Fadeev, A. Y.; McCarthy, T. J. *Langmuir* **1999**, *15*, 3759−3766. (b) We are grateful to a referee for bringing this point to our attention. The referee also noted the disparate effects of molecular scale roughness on water and hexadecane contact angles for the series of hydrocarbon silane films in ref 62a. While water values were largely insensitive to increases in molecular scale roughness, those for hexadecane increased. We have characterized effects of particulate-based roughness on water contact angles in our fluorinated system (Table 2); it would be informative to probe the response of contact angles for other liquids such as hexadecane, to compare the behavior with that studied in ref 62a. We predict that, like water, the response of hexadecane contact angles would also be different for the two systems. Such experiments will be the subject of future work.
(63) Adamson, A. W. *Physical Chemistry of Surfaces*, 4th Ed.; Wiley-Interscience: New York, 1982; pp 350−352.
(64) Menawat, A.; Henry, J.; Siriwardane, R. *J. Colloid Interface Sci.* **1984**, *101*, 110−119.
(65) Molecular modeling calculations (G. Caldwell, unpublished results) using the Dreiding force field suggest an extended length of 16 Å (silicon to trifluoromethyl fluorines) for silane **2**. Given the estimated uncertainty of ±2 Å (ref 43) for ellipsometric thicknesses measured by fixing the refractive index, we can say only that the fluorinated silane chains appear to be oriented largely normal to the surface, with a relatively small tilt angle.
(66) Everett, D. H. *Basic Principles of Colloid Science*; Royal Society of Chemistry: London, 1988.
(67) De Boer, M. P.; Knapp, J. A.; Mayer, T. M.; Michalske, T. A. *Proc. SPIE-Int. Soc. Opt. Eng.* **1999**, *3825*, 2−15.
(68) Very recent results also suggest a similar mechanism, involving deposition of both monomer and aggregate structures, for octadecyltrichlorosilane self-assembled monolayers on fused silica: Liu, Y.; Wolf, L. K.; Messmer, M. C. *Langmuir* **2001**, *17*, 4329−4335.
(69) (a) This referee questioned the mechanistic hypothesis illustrated in Figure 6, noting that equilibrium considerations argued against a scenario in which addition of gaseous water to the system induced condensation, which is formally a dehydration process. However, we note that silanol condensations can occur even in aqueous solution (ref 69b), and silanol/siloxane equilibria can lie well toward siloxane (ref 69c). On this basis we prefer our interpretation, in which the silanetriols are stabilized by hydrogen bonding in the initial monolayer (see also ref 70). However, at this point we cannot distinguish experimentally between the two alternatives, nor do we claim that the initial monolayer is free of intermolecular siloxane bonding. (b) Plueddemann, E. P. *Silane Coupling Agents*, 2nd ed.; Plenum: New York, 1991; p 57. (c) Wilczek, L.; Chojnowski, J. *Die Makromol. Chem.* **1983**, *184*, 77.
(70) Tripp, C. P.; Hair, M. L. *Langmuir* **1995**, *11*, 1215−1219. This work demonstrates that, for octadecyltrichlorosilane self-assembled films deposited from wet carbon tetrachloride, few if any siloxane bonds form between a fumed silica substrate and adsorbed silanols.
(71) **Note Added in Proof.** Close inspection of the force vs displacement trace in Figure 5b reveals that the sample was undergoing electrostatic charging upon withdrawal from the liquid. The effects of this charging can be seen as a positive (attractive) force as the bottom of the sample approached the liquid on cycles 2 and 3 (0−2 mm displacement). This general behavior has been studied previously for silanized glass surfaces immersed in water (Yaminsky, V. V.; Johnson, M. B. *Langmuir* **1995**, *11*, 4153−4158). These workers pointed out that this electrification produces a reduction in apparent advancing contact angles on subsequent immersion cycles, exactly what we see in Figure 5b. Thus, it is conceivable that the contact angle effects seen in Figure 5b are due only to static charging, rather than the humidity-induced film degradation proposed in the text. While we cannot entirely rule this out at present, we believe it to be unlikely for the following reasons. First, we have seen samples which exhibit varying degrees of electrification yet show no changes in contact angle with cycling. (For instance, the second set of three cycles in Figure 2 show slight static charging and perfectly stable contact angles.) Second, Yaminsky and Johnson note that another important result of the charging process is pronounced nonlinearity of the receding force curves, and this phenomenon is not observed in our data. Finally, the magnitude of the attractive force is significantly smaller here than in the systems studied by Yaminsky and Johnson. However, for reasons we do not currently understand, the sample in Figure 5 stored at low humidity was considerably less susceptible to static charging than was the sample stored at high humidity. This appeared consistently in our work. High humidity storage seems to have some effect on the self-assembled film itself which is not produced by low humidity exposure. These effects are irreversible; moving a sample such as that from Figure 5b from high- into low-humidity storage did not regenerate the behavior shown in Figure 5a. Obviously, more work is needed here to fully clarify the situation.